



Theoretical And Simulated Study of Wind turbine Blade profile

G. Edison, Leo D'Souza, Atul K. Saxena and Tarun V. Dodhia
School of Mechanical and Building Sciences, Vellore, Tamil Nadu, India.

ARTICLE INFO

Article history:

Received: 19 May 2013;

Received in revised form:

17 June 2013;

Accepted: 5 July 2013;

Keywords

Wind Turbine Blades,
Design Aerodynamics,
Betz Limit,
Simulated Study,
NACA Aerofoil.

ABSTRACT

This paper contains a typical wind blade design for a horizontal Axis Wind turbine. This paper deals with the parameters like blade dimension, Betz limit, calculation of coefficient of lift and coefficient of drag for the defined parameters like tip speed ratio, angle of attack, relative wind velocity, dealing with aerodynamic design principle for a wind turbine blade which includes aerofoil selection and optimal angle of attack. A simulation study has also been carried out to define certain parameters using standard NACA aerofoil for wind blade design.

© 2013 Elixir All rights reserved.

Introduction

Power has been extracted from wind over the past century with historical designs known as windmills. These were first constructed from wood, cloth and stone for general purposes like pumping water and grinding. These historical designs were highly inefficient due to their large size and bulky nature, so they were replaced in the 19th century by fossil fuel engines for the generation of power nationally. Over the past two decades, better understanding of aerodynamics and reinforced materials, particularly polymers, has led to the wind energy extraction. These turbines are used to produce electricity in bulk for industrial and domestic purposes. Over the past we have also seen that with the increasing population comes increased demand of energy. At present we are regularly facing problems with energy in terms of load shedding. So to minimize the dependency on fossil fuels, an alternative energy like wind has proven to be a boon.

By defining the orientation of shaft and rotational axis, we can classify wind turbines.

- A turbine with a shaft mounted horizontally parallel to the ground is termed a horizontal axis wind turbine (HAWT).
- Similarly, a wind turbine with a shaft mounted vertically perpendicular to the ground is termed a vertical axis wind turbine (VAWT).

Theoretical Maximum Efficiency:

$$\text{Kinetic Energy} = \text{Work} = \frac{1}{2} MV^2$$

Where:

M = mass of moving object

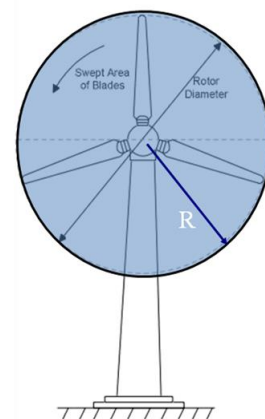
= density (ρ) x volume (Area x distance)

= $\rho \times A \times d$

= $(\text{kg/m}^3) (\text{m}^2) (\text{m})$

= kg

V = velocity of moving object



$$P = \left(\frac{1}{2}\right) \rho \cdot A \cdot V^3$$

$A = \pi R^2$ (m^2) Area of the circle swept by the rotor.

ρ = air density – in general is about 1-kg/m^3

V = Velocity of air. (m/s).

Independent to the design, there exists a physical limit for the quantity of energy that can be extracted. The kinetic energy extracted is due to the energy extraction from the wind flow over the blade profile. The reduction in air speed over the turbine gives the magnitude of energy harnessed. % extraction is not possible because it will imply zero final velocity and therefore zero flow, this is an impractical condition as total kinetic energy of wind cannot be extracted. This principle is widely accepted and indicates that the efficiency of any wind turbine does not exceed 59.3%.

We denote it by C_p (Power coefficient) = 0.593, recognised as the Betz limit.

Under this limit, it is assumed there is a constant linear velocity. Hence, any type of turbulence, wake rotation caused by drags or tip losses, which reduce the maximum efficiency further. The efficiency losses can generally be reduced by following considerations:

- Avoiding low tip speed ratios which increase wake rotation; hence, it is generally kept above 6 for HAWT.
- Use of specialised tip geometries.

Tele:

E-mail addresses: tarun.vit17@gmail.com

© 2013 Elixir All rights reserved

- Selecting a suitable aerofoil shape which can generate high lift to drag ratio.

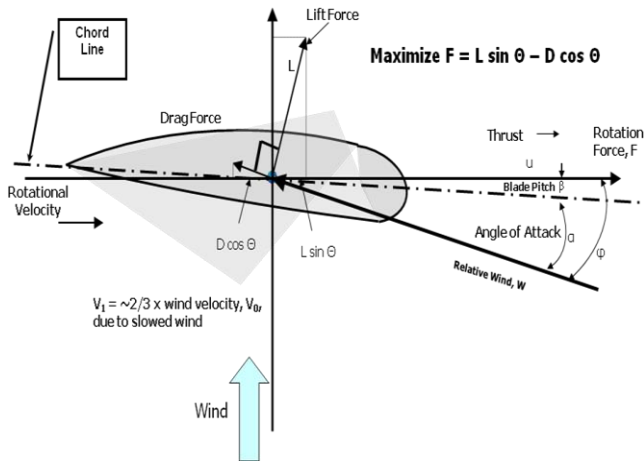
Propulsion:

For propulsion of HAWT we need to know the following equation:

$$\text{Relative wind Velocity} = \sqrt{\frac{2}{3} \text{Wind Velocity}^2 + \text{Blade Velocity}}$$

For HAWT since it is a lift driven rotar the relative velocity at which the air strikes the blade is a function of blade velocity at the radius under consideration and approximately 2/3 of the wind velocity. The relative air flow reaches the blade with an angle of incidence (θ) dependent on these velocities. The direction in which the wind is incident on the blade with respect to the angle of the blade is known as Angle of Attack.

The blade is moving rapidly and the direction of the relative wind changes with rotor speed



Blade Design:

The blades of an aeroplane propeller are curved on the front and flatter on the back towards the plane. The blade not only pulls the plane forward by the angle, but the air flow over the curve develops lift that moves the plate forward that is pull force is generated in comparison to this turbine rotors are reversed with the curve at the downwind side and with the angle of blade reversed. Here the wind will hit on the blade o the flatter side. Rotors for the wind turbines are pushed by the wind, using the lift to push them faster over the shaft. When the air stream over the blade separates due to excessive angle of attack this is known as stall condition. The disk area that is solid with blades gives the percentage of blade solidity.

$$\text{RPM} = \text{Wind speed} * \text{Tip speed ratio} * 60 / (2\pi r)$$

The aerofoil for the HAWT rotar "Lift" from the wind flowing over the blade can turn upto 12- 14 times the wind speed; the TSR of 6 is most likely.

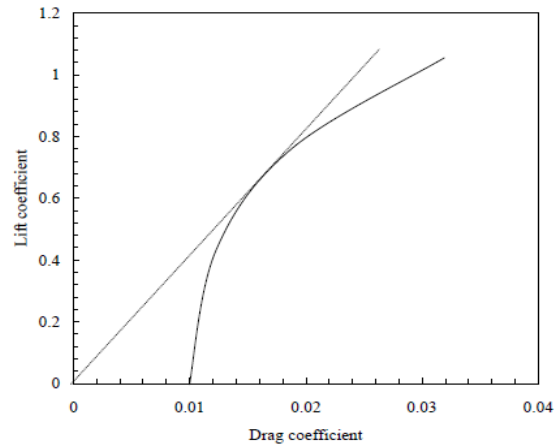
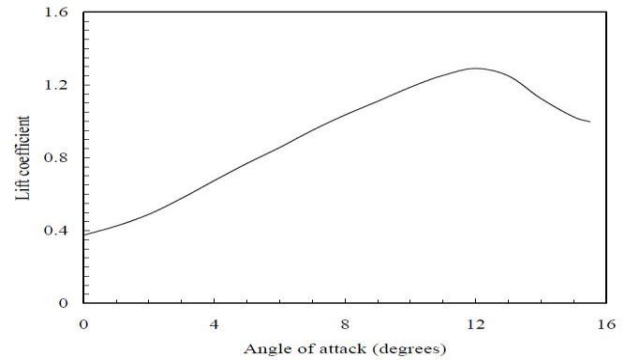
When an aerofoil is placed in the wind stream, due to the air flow on both the surfaces pressure is developed due typical curvature of the blade air that passes on the upper side travels more distance per unit time than on the lower side. Hence the air particle at the upper layer moves faster. By Bernoulli's theorem, this creates a low pressure region on the top surface of the aerofoil. The pressure difference between the two surfaces of the aerofoil results in a force. The component of this force perpendicular to the direction of the undisturbed flow is called the Lift Force. The force in the direction of the undisturbed flow (Parallel) is called Drag Force.

The lift force (L) is given by:

$$L = 0.5 * C_L * \rho * A * V^2; \quad C_L = \text{Coefficient of Lift.}$$

The Drag force (D) is given by:

$$D = 0.5 * C_D * \rho * A * V^2; \quad C_D = \text{Coefficient of Drag.}$$



Relationship between lift coefficient and drag coefficient

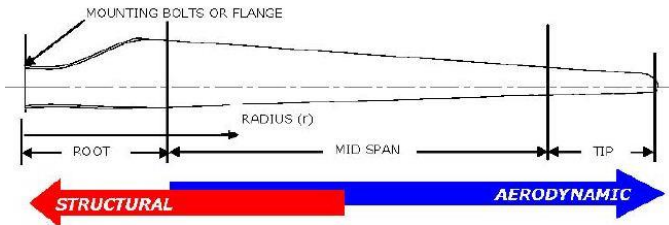
To get optimum value of angle of attack the C_D/C_L should be minimum. The drag coefficient is obtained from the C_D-C_L curve.

The lift force increases with α with lower angle of attack. As shown above int the graph Lift reaches its maximum between $12^\circ-15^\circ$ and then decreases with further increase in α . This is because at high angle of attack there is an excessive turbulent region and the boundary layers get seperated from the surface of the aerofoil in this zone, Lift force decreases and drag force increases rapidly, resulting in the stall of the blade. Hence, in any flow over an aerofoil, it is very important to place the aerofoil at an optimum angle of attack so that the C_D/C_L ratio is minimum.

Structural Blade Regions:

The modern blade can be divided into three main areas classified by aerodynamic and structural function.

- **The blade root:** It is the transition between the circular mount and the first aerofoil profile typically consist of thick aerofoil profiles with low aerodynamic efficiency— the blade profile becomes excessively large at the rotor hub as this section carries the highest loads and due to the relatively small rotor radius, it has low relative wind velocity. The low wind velocity leads to reduced aerodynamic lift leading to large chord lengths. The problem of low lift is compounded by the need to use excessively thick aerofoil sections to improve structural integrity at this load intensive region.
- **The mid span.** Aerodynamically significant—the lift to drag ratio may be maximised. Therefore utilising the thinnest possible aerofoil section that structural considerations will allow.
- **The tip.** Aerodynamically stable—the lift to drag ratio will be maximised as we move away from the root. Therefore using lean aerofoils and specially designed tip geometries to reduce noise and losses.



Simulated study:

We are using FLUENT as our computational software which gives us an computational way of checking lift and pressure contours over blade profiles. It uses the finite-volume method to solve the governing equations for a fluid. It provides the capability to use different physical models such as incompressible or compressible, inviscid or viscous, laminar or turbulent, etc. Geometry and grid generation is done using GAMBIT which is the preprocessor bundled with FLUENT.

Simulation Method:

The steps adopted for the simulations are as follows:

1. Studying and analyzing various parameters which affect the design of the blade such as Length of blade, Aerodynamic section, Plan form shape, Aerofoil thickness, Blade twist, Tip speed ratio, Chord length, relative velocity, swept area.
2. Designing the standard blade profile from the required dimensions in GAMBIT.
3. Importing the design from GAMBIT to FLUENT software to check for the parameters such as lift and drag and to analyze the flow pattern over the blade.
4. Now varying the various parameters such as chord length, chord thickness, angle of attack the lift and drag are checked for the variation.
 - a. After all iterations we get the blade with optimum values for energy extraction is obtained and analyzed further

Result:

The co-ordinates for the design of blade are given in the following table:

Standard NACA Coordinates			Design Coordinates		
1	0.0013	0	125.3	0.16289	0
0.95	0.0147	0	119.035	1.84191	0
0.9	0.0271	0	112.77	3.39563	0
0.8	0.0489	0	100.24	6.12717	0
0.7	0.0669	0	87.71	8.38257	0
0.6	0.0814	0	75.18	10.19942	0
0.5	0.0919	0	62.65	11.51507	0
0.4	0.098	0	50.12	12.2794	0
0.3	0.0976	0	37.59	12.22928	0
0.25	0.0941	0	31.325	11.79073	0
0.2	0.088	0	25.06	11.0264	0
0.15	0.0789	0	18.795	9.88617	0
0.1	0.0659	0	12.53	8.25727	0
0.075	0.0576	0	9.3975	7.21728	0
0.05	0.0473	0	6.265	5.92669	0
0.025	0.0339	0	3.1325	4.24767	0
0.0125	0.0244	0	1.56625	3.05732	0
0	0	0	0	0	0
0.0125	-0.0143	0	1.56625	-1.79179	0
0.025	-0.0195	0	3.1325	-2.44335	0
0.05	-0.0249	0	6.265	-3.11997	0
0.075	-0.0274	0	9.3975	-3.43322	0
0.1	-0.0286	0	12.53	-3.58358	0
0.15	-0.0288	0	18.795	-3.60864	0
0.2	-0.0274	0	25.06	-3.43322	0
0.25	-0.025	0	31.325	-3.1325	0
0.3	-0.0226	0	37.59	-2.83178	0
0.4	-0.018	0	50.12	-2.2554	0
0.5	-0.014	0	62.65	-1.7542	0
0.6	-0.01	0	75.18	-1.253	0
0.7	-0.0065	0	87.71	-0.81445	0
0.8	-0.0039	0	100.24	-0.48867	0
0.9	-0.0022	0	112.77	-0.27566	0
0.95	-0.0016	0	119.035	-0.20048	0
1	0.0013	0	125.3	0.16289	0

(Source: UIUC Airfoil coordinates database source dat file)

Blade Station No.	Local Radius Meters	Chord Width meters	Assumed Blade Angle
1	0.12	0.1679	14.5
2	0.24	0.1608	13.6
3	0.36	0.1537	12.7
4	0.48	0.1466	11.8
5	0.60	0.1395	10.9
6	0.72	0.1324	9.9
7	0.84	0.1253	9.1
8	0.96	0.1182	8.2
9	1.08	0.1111	7.3
10	1.2	0.104	6.3
11	1.32	0.0969	5.4
12	1.44	0.0898	4.5
13	1.56	0.0827	3.6
14	1.68	0.0756	2.7
15	1.8	0.0685	1.8

The design of the blade:

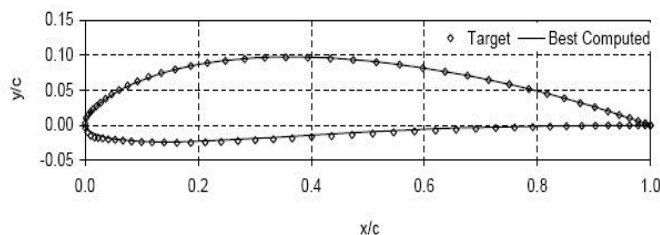


Figure: NACA (Design for importing into Gambit)

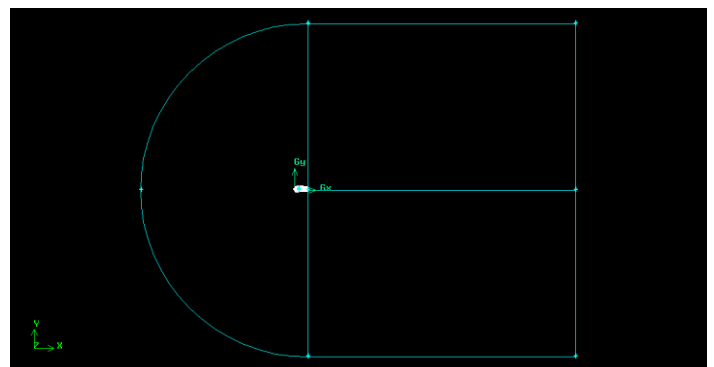


Figure: NACA Boundary Formation

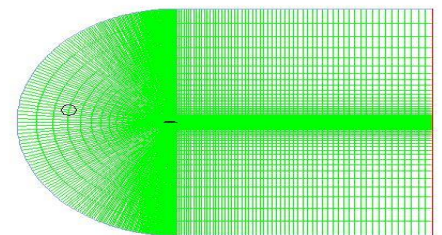
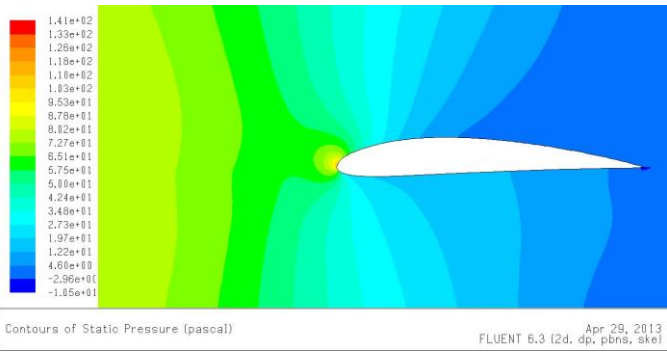
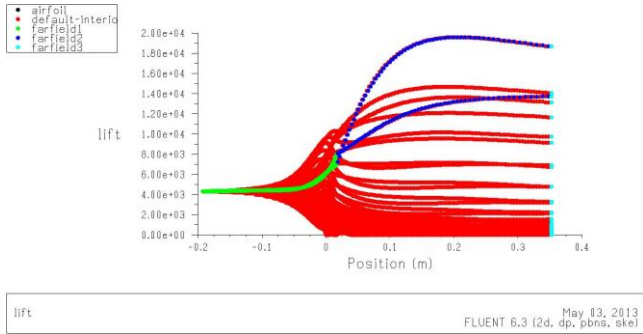


Figure: Mesh of NACA



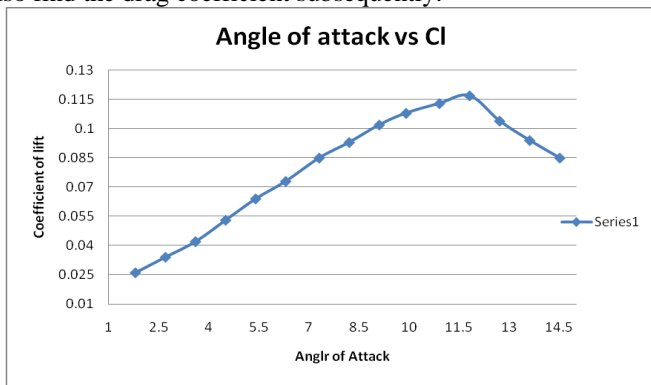
Development of high pressure region in lower surface and low pressure on top surface of airfoil with 14.5 degree angle of attack



Velocity curve for lift over the aerofoil 14.5°

The lift over the blade can be seen from the above graph. At various lengths of the blade there will be a lift generated which may be more or less depending on the aerofoil structure, inputs given to the software, flow over the body depending on predefined velocity of flow.

We use the average maximum lift generated from the above graph and plot it against the varying angle of attack. The graph generated will be more or less like the theoretical graph shown earlier. From the lift we will define coefficient of lift and we can also find the drag coefficient subsequently.



alpha	Cl
14.5	0.085
13.6	0.094
12.7	0.104
11.8	0.117

10.9	0.113
9.9	0.108
9.1	0.102
8.2	0.093
7.3	0.085
6.3	0.073
5.4	0.064
4.5	0.053
3.6	0.042
2.7	0.034
1.8	0.026

Conclusion

After the study performed it is noted that we can calibrated any blade profile using a standard NACA profile, to generate user requires coordinates by trial and error method and check the pressure flow pattern over the airfoil to generate a suitable lift drag over the airfoil and compute the following by generating lift curve against angle of attack. Lift generated by this method in these results is always an approximate. The results are seen to be converging with high pressure zone on flatter end of blade and low pressure developed on upper surface of airfoil surface. The theoretical aspect help us to understand the aerodynamics and different factors affecting the blade profile while the simulated study gives us a better visionary aspect of what is actually happening over the blade profile by generating curves and flow patterns.

The velocity curve will help in calculating the lift required.

References

- [1]. Buhl ML (2000) WT- PERF user’s guide. NREL
- [2]. Dahl KS (1999) Experimental verifications of the new RISO-A1 airfoil family for wind turbines. In: Proceedings of EWEC’99, pp 85-88
- [3]. Dini P, Coiro DP, Bertolucci S (1995) Vortex model for airfoil stall prediction using an interactive boundary layer method. In: Wind Energy 1995, SED and American Society of Mechanical Engineers
- [4]. Eggleston DM, Starcher KL (1990) A comparative study of the aerodynamics of several wind turbines using flow visualization. J. Solar Energy Engineering 112:301-309
- [5]. Hansen AC, Butterfield CP (1993) Aerodynamics of horizontal -axis wind turbines. Annual Review of Fluid Mechanics 25: 115-149
- [6]. Koleffler RG, Sitz EL (1946) Electrical energy from winds. (Kansas State College of Engineering, Experiment Station Bulletin 52, Manhattan, Kansas).
- [7]. Lysen EH (1982) Introduction to wind energy. CWD, Netherlands
- [8]. Mathew S (1990) Design, fabrication and testing of a Savonius rotor with deflector augmentor. M.Tech. thesis, Kerala Agricultural University
- [9]. McCarty J (1993) PROP93 User’s Guide. Alternative Energy institute.